

Assessing the Raspberry Pi as a low-cost alternative for acquisition of near infrared hemispherical digital imagery

Kirby, Jennifer; Chapman, Lee; Chapman, Victoria

DOI:

[10.1016/j.agrformet.2018.05.004](https://doi.org/10.1016/j.agrformet.2018.05.004)

License:

Creative Commons: Attribution-NonCommercial-NoDerivs (CC BY-NC-ND)

Document Version

Peer reviewed version

Citation for published version (Harvard):

Kirby, J, Chapman, L & Chapman, V 2018, 'Assessing the Raspberry Pi as a low-cost alternative for acquisition of near infrared hemispherical digital imagery', *Agricultural and Forest Meteorology*, vol. 259, pp. 232-239. <https://doi.org/10.1016/j.agrformet.2018.05.004>

[Link to publication on Research at Birmingham portal](#)

Publisher Rights Statement:

Published in *Agricultural and Forest Meteorology* on 15/05/2018

DOI: <https://doi.org/10.1016/j.agrformet.2018.05.004>

General rights

Unless a licence is specified above, all rights (including copyright and moral rights) in this document are retained by the authors and/or the copyright holders. The express permission of the copyright holder must be obtained for any use of this material other than for purposes permitted by law.

- Users may freely distribute the URL that is used to identify this publication.
- Users may download and/or print one copy of the publication from the University of Birmingham research portal for the purpose of private study or non-commercial research.
- User may use extracts from the document in line with the concept of 'fair dealing' under the Copyright, Designs and Patents Act 1988 (?)
- Users may not further distribute the material nor use it for the purposes of commercial gain.

Where a licence is displayed above, please note the terms and conditions of the licence govern your use of this document.

When citing, please reference the published version.

Take down policy

While the University of Birmingham exercises care and attention in making items available there are rare occasions when an item has been uploaded in error or has been deemed to be commercially or otherwise sensitive.

If you believe that this is the case for this document, please contact UBIRA@lists.bham.ac.uk providing details and we will remove access to the work immediately and investigate.

1 **Title:** Assessing the Raspberry Pi as a low-cost alternative for acquisition of near
2 infrared hemispherical digital imagery

3

4 **Authors & Affiliations:**

5 Jennifer Kirby

6 University of Birmingham, College of Geography, Earth and Environmental Science,
7 Edgbaston, Birmingham, B15 2TT, JXK067@bham.ac.uk

8 Professor Lee Chapman (Principle Correspondence)

9 University of Birmingham, College of Geography, Earth and Environmental Science,
10 Edgbaston, Birmingham, B15 2TT, l.chapmam@bham.ac.uk

11 Dr Victoria Chapman

12 Met Office Surface Transport Team, Birmingham Centre for Railway Research and
13 Education, Gisbert Kapp Building, University of Birmingham, Edgbaston,
14 Birmingham, B15 2TT, victoria.chapman@metoffice.gov.uk

15

16 'Declarations of interest: none'

17

18 **Abstract**

19 Hemispherical imagery is used in many different sub-fields of climatology to calculate
20 local radiation budgets via sky-view factor analysis. For example, in forested
21 environments, hemispherical imagery can be used to assess the leaf canopy, (i.e.
22 leaf area / gap fraction) as well as the radiation below the canopy structure. Nikon
23 Coolpix cameras equipped with an FC-E8 fisheye lens have become a standard
24 device used in hemispherical imagery analysis however as the camera is no longer
25 manufactured, a new approach needs to be investigated, not least to take advantage
26 of the rapid development in digital photography over the last decade. This paper
27 conducts a comparison between a Nikon Coolpix camera and a cheaper alternative,
28 the Raspberry Pi NoIR camera, to assess its suitability as a viable alternative for
29 future research. The results are promising with low levels of distortion, comparable to
30 the Nikon. Resultant sky-view factor analyses also yield promising results, but
31 challenges remain to overcome small differences in the field of view as well as the
32 present availability of bespoke fittings.

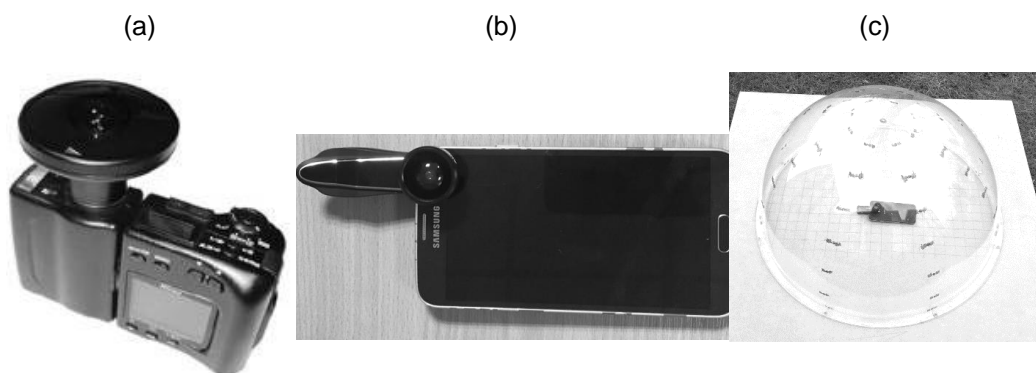
Comment [JK1]: Removed resolution comment

33 **Key words:** Hemispherical fisheye, Near infra-red, Raspberry Pi, Sensors

34 **1. Introduction**

35 Hemispherical imagery is commonly used to assist in the assessment of radiation
36 budgets. Examples of use include below tree canopies, in urban areas or within
37 riverine environments (*Hall et al., 2017; Liu et al., 2015; Chapman, 2007; Chapman*
38 *et al; 2007; Bréda, 2003; Ringold et al., 2003; Watson and Johnson, 1987*). Imagery
39 is usually obtained using a camera equipped with a fisheye lens (Figure 1a) which
40 allows the camera to take an approx. 180° hemispherical image (*Liu et al., 2015;*
41 *Chianucci et al., 2015*). These images are then processed to analyse the amount of

42 visible sky shown in the image (known as the sky-view factor). This can then be used
43 in forestry research to quantify the health of a tree and to compare differences
44 between tree canopies (*Schwalbe et al., 2009; Leblanc et al., 2005; Jonckheere et al.*
45 *2004*).



46 Figure 1 (a) FC-E8 Fisheye lens attached to a Coolpix camera Source: Reproduced
47 with permission from Chapman et al. (2007), copyright © 2007 IEEE, (b) First2Savv
48 1850 fisheye camera attached to a Samsung Galaxy S5 Neo; (c) Perspex Dome
49 used to measure distortion.

50 The use of fisheye imagery for this application can be dated back to the early work of
51 Anderson (1964), but it was the advent of digital photography which saw the
52 approach become widely adopted. Following a number of scoping studies, which
53 successfully compared results obtained from film cameras to the new generation of
54 digital cameras (*Englund et al. 2000; Frazer et al. 2001; Hale and Edwards, 2002*),
55 the new technology quickly became adopted by the scientific community. However,
56 following the successful transition to mass digital photography, studies for the past
57 two decades have become very reliant on the early digital cameras produced by
58 Nikon (**Error! Reference source not found.**) such as the Coolpix 950 or 4500
59 (*Chianucci et al. 2016; Lang et al., 2010; Chapman, 2007; Zhang et al., 2005; Baret*

60 *and Agroparc, 2004; Ishida, 2004*). Indeed, whilst research into hemispherical
 61 imagery has also been conducted using alternative cameras and equipment (Table
 62 **2Error! Reference source not found.**), the Nikon Coolpix range equipped with the
 63 FC-E8 fisheye lens undoubtedly remains the most popular choice in research to
 64 date.

<i>Seasonal Changes in Canopy Structure</i>	
<i>Liu et al., 2015</i>	Used a Nikon Coolpix 4500 camera at sunset / sunrise to capture hemispherical images of tree canopies in order to investigate seasonal changes of tree canopies.
<i>Comparing Nikon Coolpix to film cameras and Leaf canopy analysers</i>	
<i>Homolová et al., 2007</i>	Used a Nikon Coolpix 8700 to compare canopy analysers to hemispherical imagery.
<i>Garrigues, et al., 2008</i>	Compares Nikon Coolpix 990 with LAI-2000 and AccuPAR.
<i>Frazer et al., 2001</i>	Compared a Nikon 950 to a film camera and highlighted the potential for blurred edges and colour distortion of a Coolpix camera but noted it can be used in calculating canopy gap measurements.
<i>Englund et al., 2000</i>	Compared a digital Nikon 950 and a film camera to find that low resolution images from the Nikon 950 were an adequate comparison to film cameras.
<i>Grimmond et al., 2001</i>	Compared a Nikon 950 Coolpix to a plant canopy analyser and found that the Nikon was an effective and easy approach to canopy analysis.

<i>Gap function Analysis and Estimation of tree canopies</i>	
<i>Hu et al., 2009</i>	Uses a Nikon 950 Coolpix camera to take hemispherical images to calculate gap size and shape within a tree canopy.
<i>Gap function Analysis and Estimation of tree canopies</i>	
<i>Zhang et al., 2005</i>	Researched the effect of exposure on calculating the leaf area index and gap function analysis using a Nikon Coolpix 4500.
<i>Lang et al., 2010</i>	Calculated gap function of canopies using a Nikon Coolpix 4500 and compared it to the Canon EOS 5D cameras.
<i>Chianucci et al. 2016</i>	Used a Nikon 4500 to compare gap functions in forested canopies.
<i>Danson et al., 2007</i>	A Nikon 4500 was used as a comparison to terrestrial laser scanning.
<i>Adaption or calibration of Nikon cameras</i>	
<i>Chapman, 2007</i>	Adapted a Nikon 4500 camera to make in near infra-red in order to better estimate sky-view factors and the woody bark index of tree canopies.
<i>Baret, & Agroparc, 2004</i>	Used a Nikon 4500 in order to determine the optical centre of an image using a fisheye lens.
<i>Ishida, 2004</i>	Created threshold software for colour images from a Nikon 950 camera.

65 Table 1 List of sample studies that use Nikon Coolpix cameras.

Studies	Camera used	Approach
<i>Kelley and Krueger, 2005</i>	HemiView 2.1 digital image system	Used a 20-megapixel SLR CMOS camera as part of the HemiView software (Delta Devices 2017) to record canopy structure in riparian environments
<i>Duveiller and Defourny, 2010</i>	Canon PowerShot A590 camera	Used a Canon PowerShot A590 camera to assess batch processing of hemispherical images
<i>Rich, 1990</i>	Canon T90 Minolta X700 Nikon FM2 Olympus OM4T	Comprehensive instructions on how to take hemispherical photography with a list of cameras suitable for research
<i>Urquhart, et al., 2014</i>	Allied Vision GE-2040C camera	Uses sky-view factors from a high dynamic range camera to calculate short term solar power forecasting
<i>Wagner and Hagemeyer, 2006</i>	Canon AE-1 camera	Used a Canon camera to estimate leaf inclination angles on tree canopies

67 Table 2 Studies using alternative cameras for hemispherical photography.

68

69 The Nikon Coolpix range of cameras remains a key tool in forest climatology (**Error!**70 **Reference source not found.** and Table 2**Error! Reference source not found.**).71 Unfortunately, the Coolpix range is no longer readily available (*Nikon, 2016*) with

72 digital camera technology advancing considerably in the interim making models such

73 as the Coolpix 4500 camera appear large and bulky with a relatively poor battery life
74 and low image resolution (3.14 megapixels). However, even today, the FC-E8
75 fisheye lens remains one of the least distorted on the market (*Holmer et al.*, 2001)
76 and as such, the camera series remains very popular with researchers as a tried and
77 tested means to collect hemispherical imagery (*Chapman, 2007*). A significant
78 further advantage of the Coolpix range of cameras was the ability to easily convert
79 the camera to take near infra-red (NIR) imagery. By adapting a camera in this way, it
80 significantly enhances its functionality in the forest environment as due to the highly
81 reflective nature of vegetation it becomes easier to distinguish this from woody
82 elements and other features in imagery when taken in NIR; which can then be used
83 to assess the health and density of tree canopies (*Chen et al.*, 1996; *Turner et al.*,
84 1999).

85 Overall, the Nikon Coolpix camera has reached the point where it is informally
86 viewed as a standard device for this purpose, but with dwindling numbers now
87 available for purchase on internet auction sites, there is a need to investigate new
88 and more sustainable means to collect data in the long term. **Whilst new digital**
89 **cameras are available on the market, the** approach explored in this paper is to
90 investigate whether a low-cost alternative can be developed using readily available
91 off-the-shelf components.

92 **2. Methods**

93 **2.1 Adapting a Raspberry Pi**

94 The Raspberry Pi is a range of small computers designed to minimise the cost of
95 computing and thus make it, and computer programming more generally, accessible
96 to a wide audience. After a prolific launch, it now has a worldwide following of

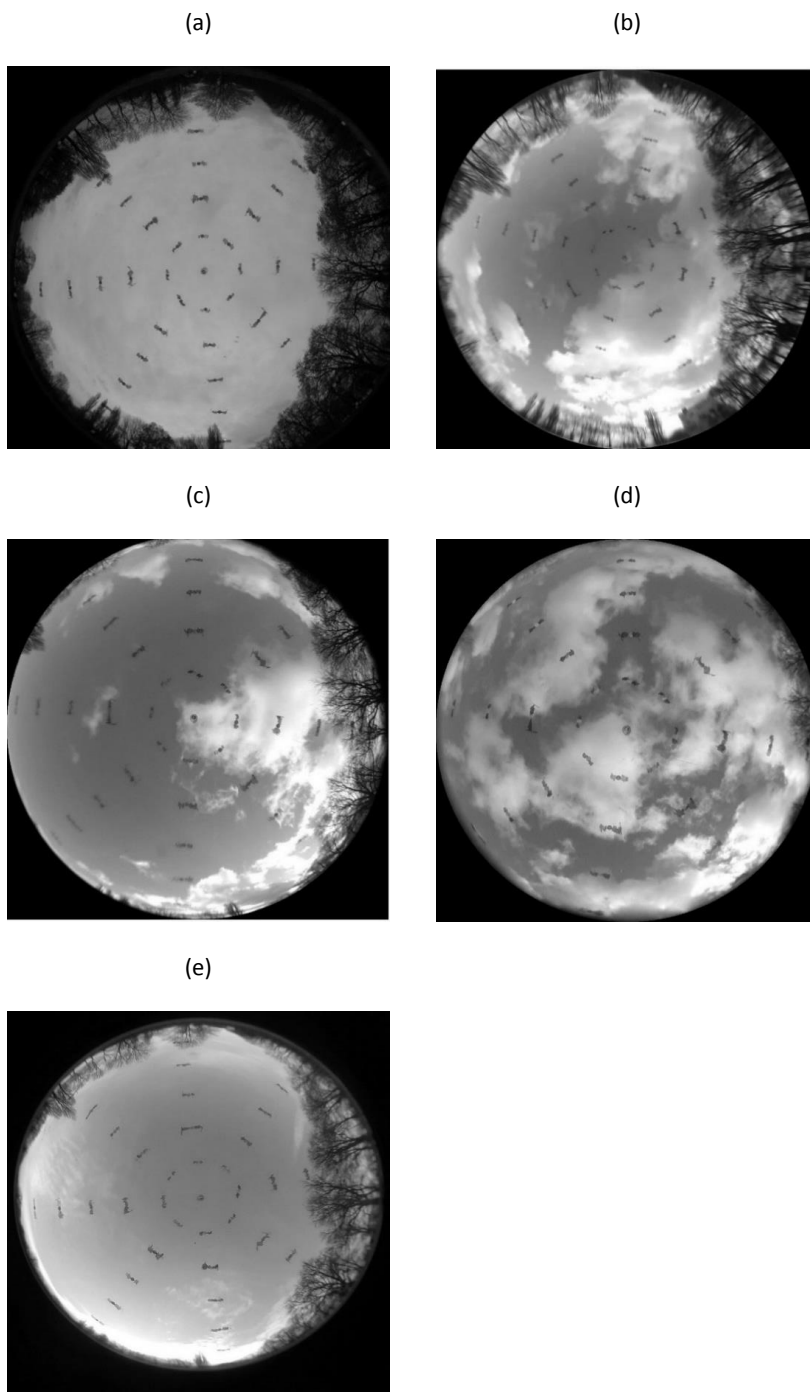
97 developers focussed on producing generic code and peripherals for use in a range of
98 applications. As an example, the computer can now be readily fitted with a
99 Raspberry Pi camera and subsequently programmed to take images at set time
100 intervals.

101 At the time of writing, the most popular Pi compatible camera available on the market
102 is the Pi camera which comprises of a Sony IMX219 9-megapixel sensor. This is
103 available either as a standard device or as a Pi NoIR camera where the infra-red
104 blocking filter (needed by modern digital cameras due to the inherent capability to
105 see beyond the visible spectrum: *Chapman, 2007*) has been removed (*Raspberry Pi,*
106 *2016*). As outlined in the previous section, NIR capability improves the utility of the
107 approach for use in forested environments.

108 **2.2 Comparison of Fisheye lenses**

109 Unfortunately, a fisheye lens is presently not available that has been specifically
110 designed for the Pi NoIR camera. However, due to the recent proliferation of
111 smartphone photography, there is a wide range of fisheye lenses that are now
112 available for smartphones which have the potential to be used. The key
113 consideration here, as per Holmer et al, (2001), is to select a lens with minimal
114 distortion to reduce error in later image analyses. This can be achieved by testing
115 the equiangularity of the lens by calculating any distortions in the radial distance. As
116 shown in Figure 2, the aim is to acquire an image where the radial distance is
117 directly proportional to the zenith angle (*Chapman, 2008*).

118



119 Figure 2 (a) Visual comparison of Nikon Coolpix camera, (b) smart phone camera
 120 with attached 185° fisheye lens, (c) smart phone camera with attached fisheye lens

121 198°, (d) smart phone camera with attached fisheye lens 180° and (e) smart phone
122 camera with attached fisheye lens 235°

123

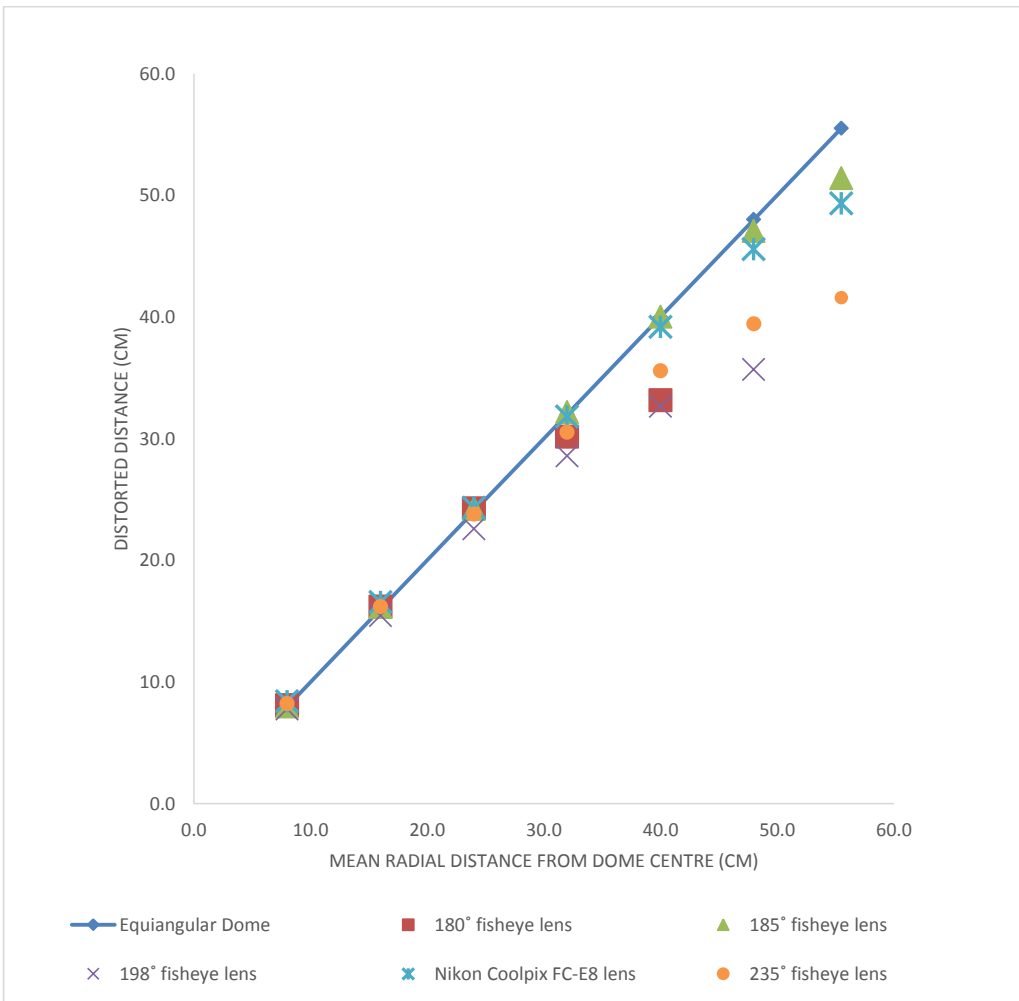
124 A range of available fisheye lenses were tested for distortions (Table 3). In this initial
125 test, the fisheye lenses were clipped onto a Samsung Galaxy S5 Neo (Figure 1 b)
126 and placed under a large Perspex calibration dome marked at equal points along the
127 sides using a compass (Figure 1 c). A plumb bob was then used to position the
128 device directly below the centre of the dome before a series of images collected
129 (Figure 2). Measurement distortions were then calculated using Image-J software
130 (Figure 3).

131

Product	Field of view	Cost (At time of writing)
Yarrashop fisheye lens	180	£7.99
First2Savv JTSJ-185-A01 fisheye lens	185	£8.99
AUKEY fisheye lens	198	£11.99
MEMTEQ universal fisheye lens	235	£10.99

132 Table 3 Mobile fisheye lenses specification.

133



134

135 Figure 3 Comparison of radial distortion between different mobile fisheye lenses and

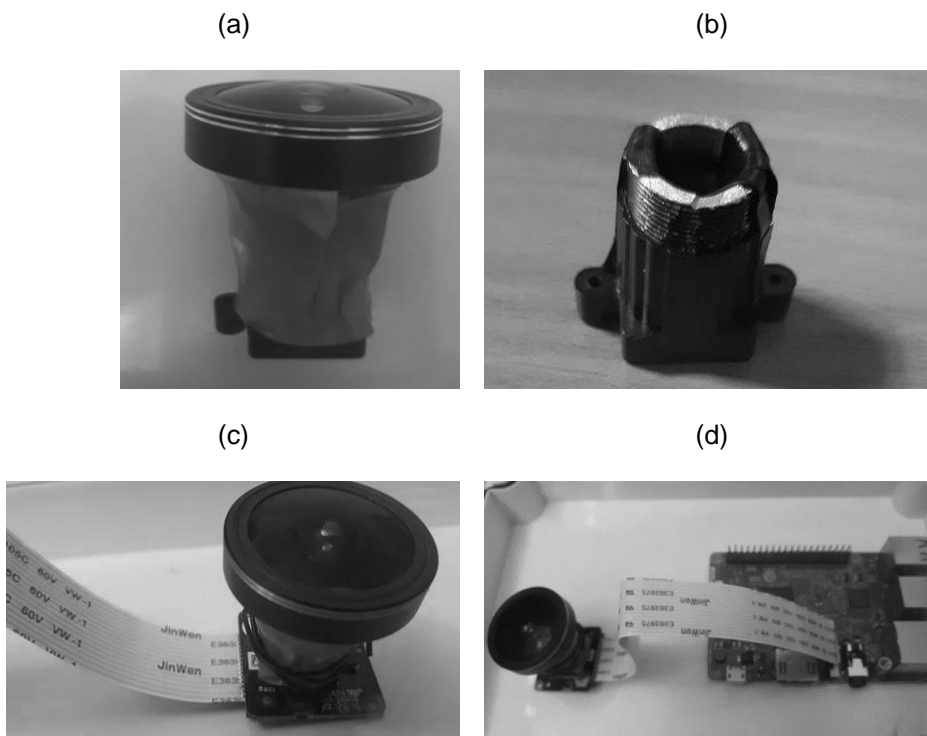
136 Nikon Coolpix 4500 camera FC-E8 lens.

137

138 The results show that the 185° fisheye lens (Figure 2b) is most comparable with the
139 Nikon Coolpix FC-E8 lens (Figure 2a). It has a similar field of view (FOV) and
140 despite a slight reduction in image clarity at high radial distances, the 185° lens has
141 the lowest level of distortion (Figure 3). However, comparisons between the Nikon
142 Camera FC-E8 lens and other mobile fisheye lenses are not as favourable and all
143 display clear distortions and/or significant reductions in FOV. For example, the 180°
144 (Figure 2d) camera captures the lowest FOV of the compared fisheye lenses (Figure
145 3). The 198° fisheye lens (Figure 2c) has excellent clarity at high radial distances
146 however has a lower FOV then reported and high levels of distortion (Figure 3).
147 Conversely, the 234° fisheye lens (Figure 2e) has a high FOV however has high
148 levels of distortion, especially at high radial distances (Figure 3). Based on these
149 analyses, the 185° fisheye lens was chosen for further investigation.

150 **2.3 Adapting a Pi Noir camera to take hemispherical images**

151 In order to use the 185° fisheye lens with the Pi NoIR camera, a series of small
152 adaptations are required. Whilst these adaptations could be achieved using 3D
153 printing technology, this was achieved in this study using parts scavenged from the
154 First2Savv 185° fisheye lens (Figure 4Error! Reference source not found.a) and
155 tubing from a Waveshare Raspberry Pi Camera Module Kit (Figure 4b). The camera
156 component of the Waveshare kit was removed, using a saw and drill, to leave a
157 hollow tube. The tubing (Figure 4b) was then tied and secured to the base of the
158 Raspberry PI NoIR camera using thin wire (Figure 4c). The camera was then
159 attached to the Raspberry Pi board using the connector port (Figure 4d).



160 Figure 4 (a) 185° fisheye lens attached to base (b) base component of Raspberry Pi
 161 fisheye module, (c) fisheye module attached to Raspberry Pi NoIR camera (d)
 162 Camera module attached to a Raspberry Pi computer.

163

164 3. Comparison of Nikon camera and Pi NoIR Raspberry Pi camera.

165 3.1 General Specifications

166 Table 4 shows the specification comparison of both the Pi NoIR camera version 1
 167 and 2, the Nikon Coolpix 4500 and the Nikon Coolpix 9000 camera. As has been
 168 demonstrated in the previous section, the reported FOV can vary with individual
 169 cameras (*Grimmond et al., 2001*) and therefore this has been estimated in this study
 170 using a mechanical clinometer. The adapted Pi camera FOV (164°) is less than the

Comment [JK2]: Removed resolution argument

171 Nikon Coolpix FOV (176°) which is hypothesised to be a consequence of the added
 172 tubing (Figure 4b) causing some distortion and loss of image at ground level.

	Nikon 900	Nikon 4500	Pi NoIR V1	Pi NoIR V2
Pixel range	1.2 megapixels	3.14 megapixels	5 megapixels	8 megapixels
Optical Zoom	3 x optical zoom lens	4 x optical zoom lens	N/A	N/A
Field of View	183° FC-E8 lens (176° using a mechanical clinometer)	183° FC-E8 lens (176° using a mechanical clinometer)	185° mobile fisheye lens (164° using a mechanical clinometer)	185° mobile fisheye lens (164° using a mechanical clinometer)
Dimensions	143 x 76.5 x 36.5mm (5.6 x 3.0 x 1.4 in.)	130 x 73 x 50mm (5.1 x 2.9 x 2.0 in.)	25 x 24 x 1mm	25 x 24 x 1mm
Cost	£100*	£200*	£25	£25

173 * Approximate Second-hand price

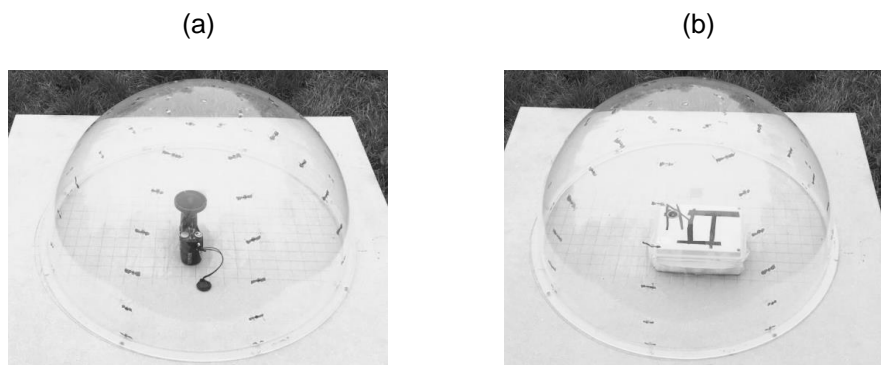
174 Table 4 Comparison of Coolpix cameras to Raspberry Pi cameras

175

176 **3.2 Distortion Analysis**

177 As hemispherical imagery is mostly used in the analysis of tree canopies, the loss of
 178 information at ground level (i.e. high radial distances) is less of a concern. It is at
 179 these extremities of the image where distortions are also more common and indeed
 180 one of the main attractions of the Nikon Coolpix range of cameras (*Holmer et al.*,

181 2001). Whilst an equiangular lens is not an essential requirement of a camera
182 system for this application, it does ensure fewer corrections are required and
183 minimises error in subsequent analysis. The distortions of the adapted fisheye lens
184 are again tested by using the Perspex calibration dome (Figure 5).



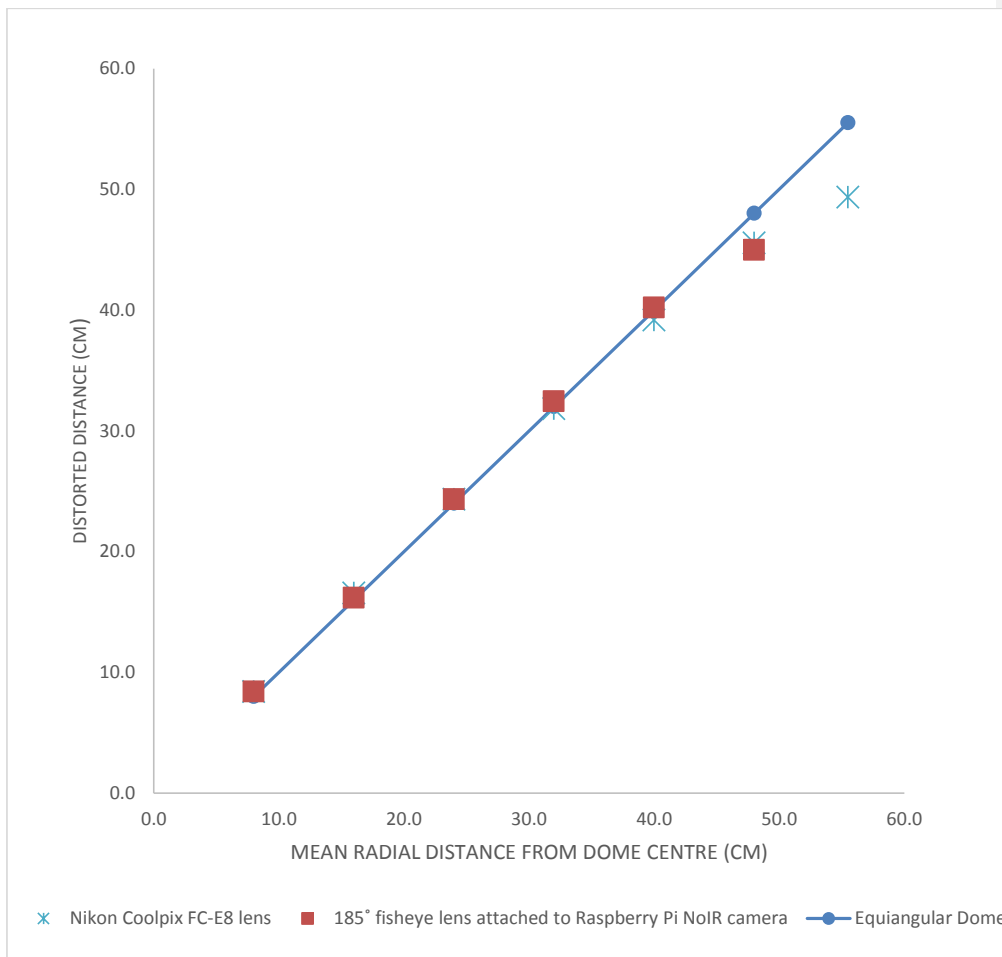
185 Figure 5 (a) Nikon Coolpix camera in a Perspex dome and (b) Raspberry Pi NoIR
186 camera with fisheye attached under Perspex dome.

187
188 The FOV of the adapted Pi camera is demonstrated to be less than the Nikon
189 camera however there is a greater level of distortion when using a Nikon Coolpix
190 camera (

191). This difference is likely due to the size of the equipment with the Nikon Coolpix
192 camera being larger in size than the Pi camera lens (145 mm compared to 25mm).
193 With respect to equiangularity, there is a strong correlation between radial distance
194 distortions of the Nikon Coolpix FC-E8 lens camera and Raspberry Pi NoIR adapted
195 fisheye camera at 99.9% confidence level (

196).

197



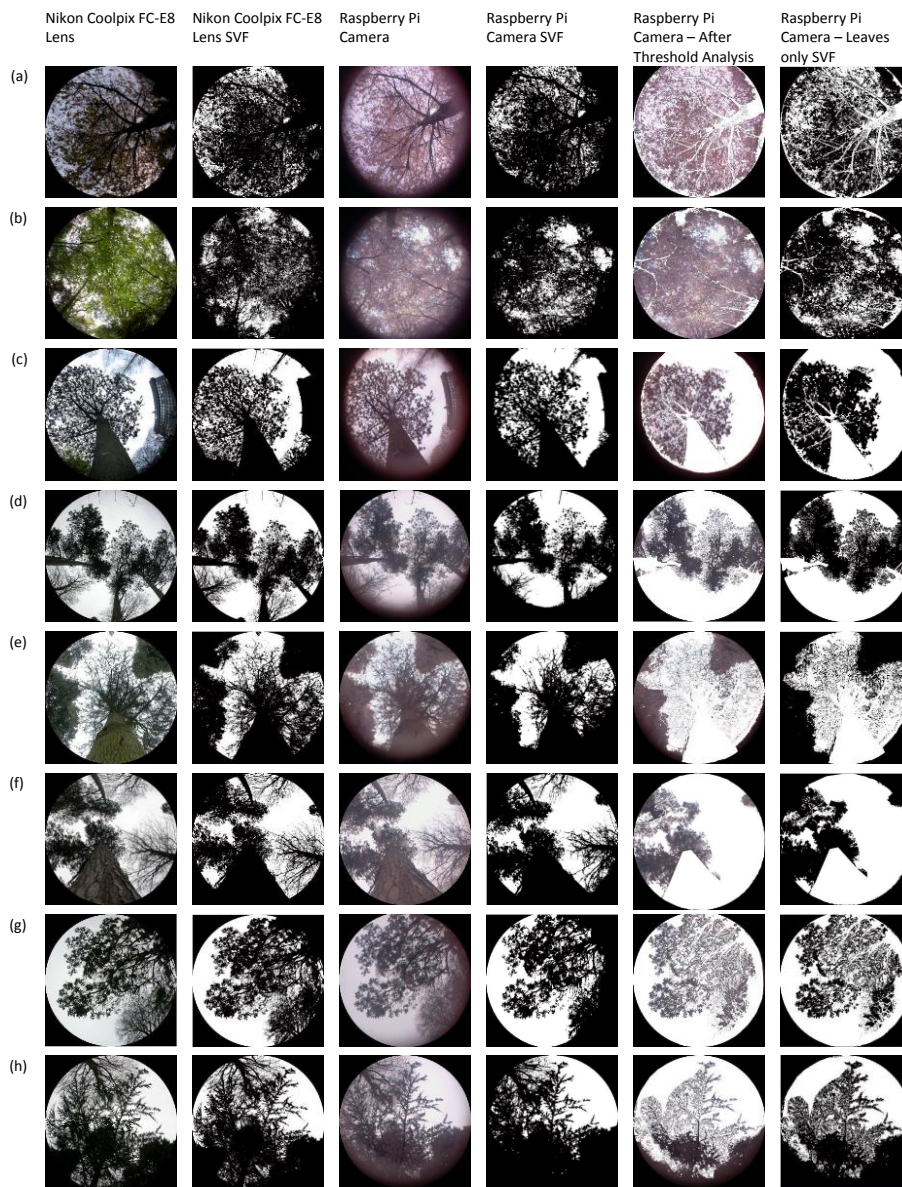
198

199 Figure 6 Radial Distortion of a Nikon Coolpix FC-E8 lens camera and a Raspberry Pi
200 camera with attachable fisheye lens.

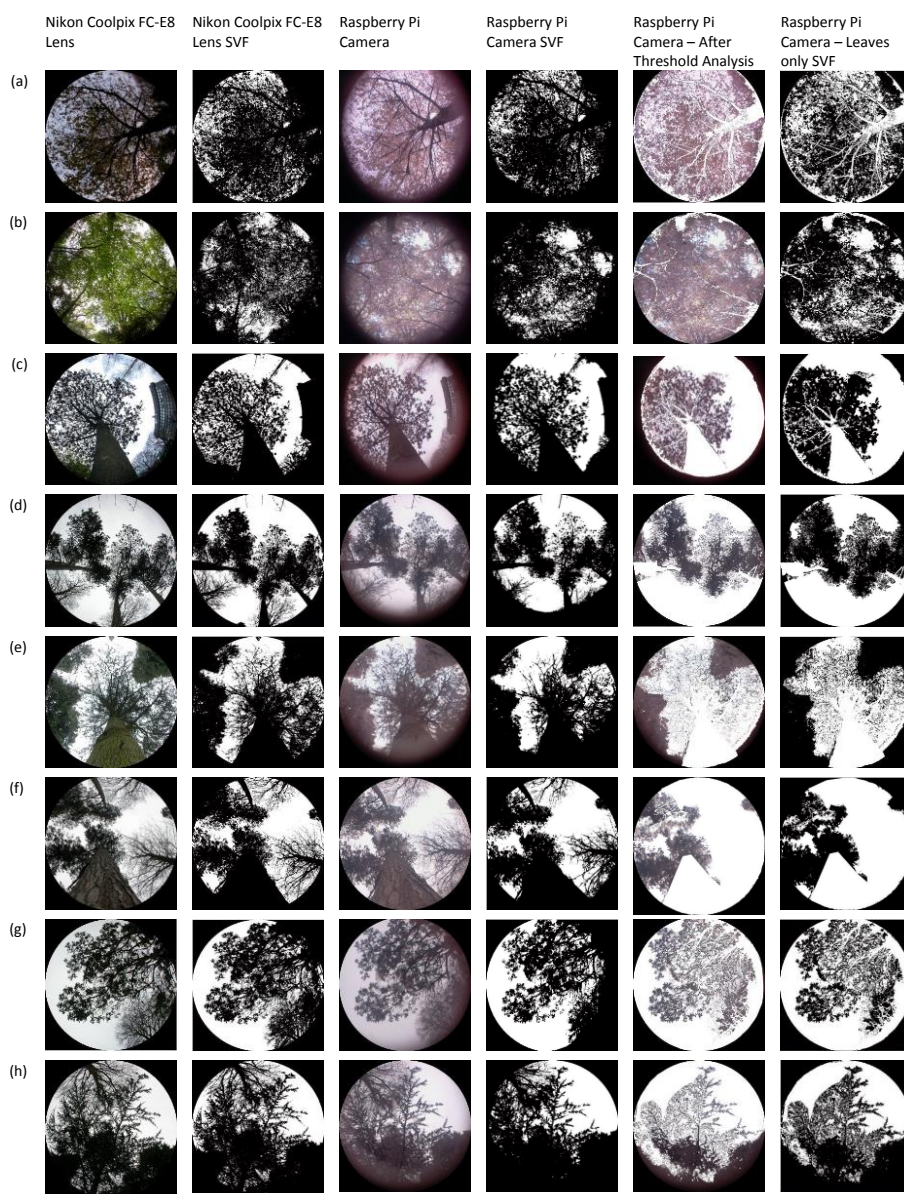
201

202 **3.3 Sky-view factor Analysis**

203 **To further demonstrate the inter-device comparability, images were captured**
204 **devices for sky-view factor analysis (**

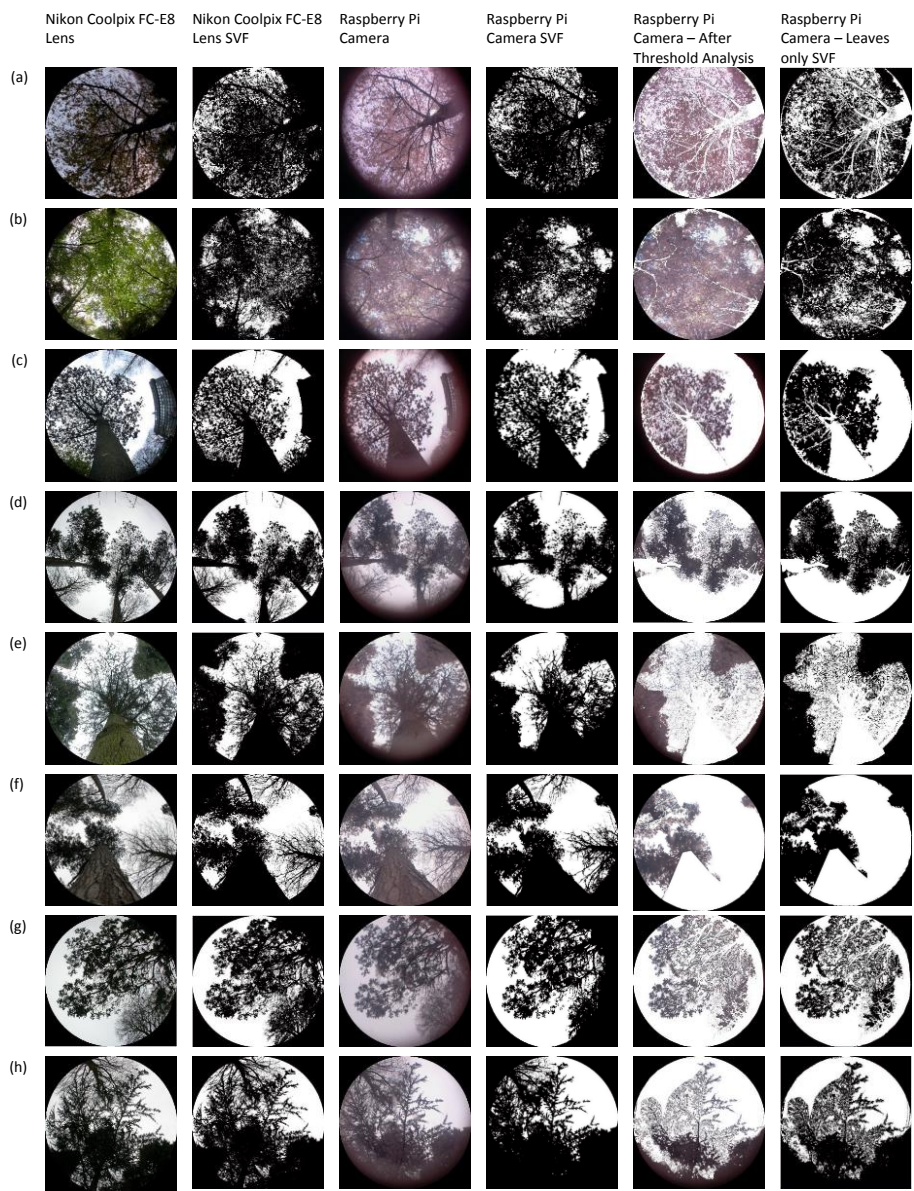


206 Figure 7). The Images were then analysed using 'Sky-View Calculator' software
 207 (Göteborg Urban Climate Group, 2018) developed by Lindberg and Holmer
 208 (2010) using a process where the image was converted to binary (



209
 210 Figure 7), divided into concentric annuli before calculating the number of white Pixels
 211 (sky) in each annulus and summed (Holmer et al. 2001; Johnson and Watson, 1984;

212 *Steyn 1980*). Analyses were performed on the original imagery as well as images
 213 cropped to have the same FOV. Table 5 shows that when the FOV is uncorrected,
 214 the Pi overestimates the sky-view factor, but when this is corrected, the output is
 215 very similar and is significant at the 99.9% level.



217 Figure 7 Visual variations in sky-view factors when comparing a Nikon Coolpix FC-
 218 E8 lens with a 185° Raspberry Pi NoIR camera.

Comment [JK3]: Changed an to a

219

Image	Sky-view factor			Leaf-view factor
	Nikon Coolpix Camera (Non-adjusted FOV)	Nikon Coolpix Camera (adjusted FOV)	Raspberry Pi Camera.	
(a)	0.25	0.17	0.17	0.55
(b)	0.24	0.26	0.29	0.68
(c)	0.40	0.42	0.44	0.45
(d)	0.4	0.45	0.45	0.45
(e)	0.3	0.34	0.35	0.26
(f)	0.4	0.45	0.47	0.33
(g)	0.37	0.40	0.44	0.42
(h)	0.48	0.33	0.34	0.53

220 Table 5 Sky view factors of Nikon Coolpix camera adjusted FOV, Raspberry Pi NoIR
 221 camera, Nikon Coolpix unadjusted FOV and Raspberry Pi leaves only images.

222

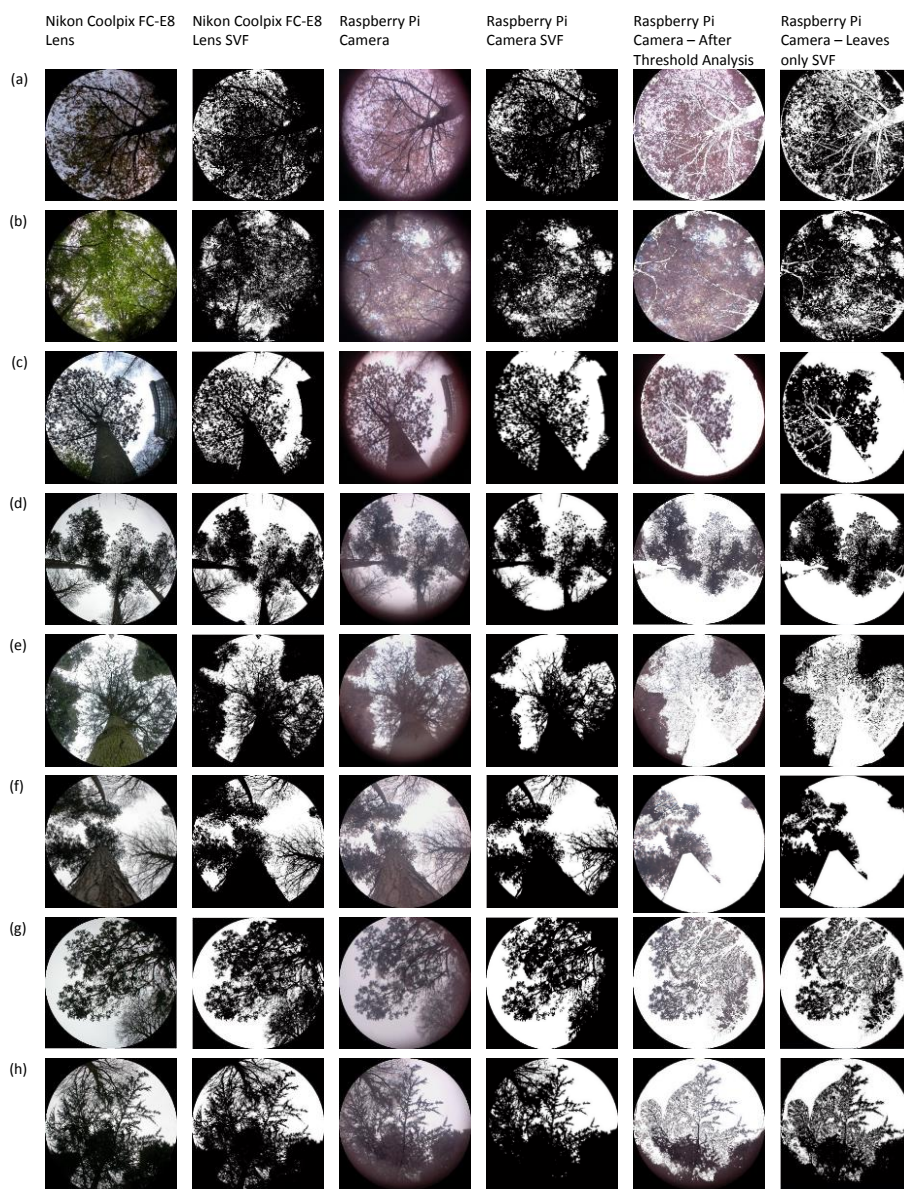
223 3.4 Near Infrared Capabilities

224 In addition to hardware availability, the advantages of using a Raspberry Pi NoIR
 225 camera over a Nikon 4500 camera is the in-built near infra-red (NIR) technology.

Comment [JK4]: Removed resolution argument

226 Although it is also possible to convert the Nikon Coolpix camera to take NIR images
227 (*Chapman, 2007*), this involves substantial effort which risks damaging the camera.

228 **The capability of the Pi NoIR was confirmed in this study. A simple threshold**
229 **analysis proved sufficient to remove all other aspects of the image except for**
230 **vegetation (**



232 Figure 7Table 5). The differences in sky-view factor can then be calculated; from
233 this a leaf-view calculation were made and presented in Table 5, indicating an
234 approximation of leaf cover in the image and further highlights the utility of the
235 camera in forestry applications.

236 4. Conclusions

237 The Nikon Coolpix camera range has provided a reliable 'standard' solution for
238 obtaining hemispherical fisheye imagery for many years. However, whilst still fit for
239 purpose, an alternative is needed to ensure a sustainable means of data collection
240 moving forward. This paper has shown that comparable results can be provided with
241 a low-cost image collection system using readily available components.

Comment [JK5]: Removed resolution comment

242 The Pi NoIR camera provides an off-the-shelf NIR solution, making it perfect for use
243 in forested environments and thus removing the need for further adaptation (i.e.
244 removal of blocking filters and addition of cold mirrors: *Chapman, 2007*). However,
245 fisheye lenses are not yet readily available and hence there is presently a need to
246 carry out alternative adaptations such as those outlined in this paper, or the use of
247 simple 3D printing technology. However, the most positive result from this study is
248 the direct comparability of the imagery (and subsequent results from sky-view factor
249 analyses) obtained from the two techniques. Both systems have similarly low levels
250 of distortion, but there are minor differences in relation to the FOV. Further research
251 is needed to adapt the Raspberry Pi to make the sensor usable in the field; this
252 includes waterproofing the technology and testing the equipment at various
253 temperature ranges. A limitation of this study is that the technology was not tested
254 for interference from electronic or radio waves.

255

256 Further advantages of the Raspberry Pi approach are the computing capability of the
257 device, which means it has internal logging capabilities and (once waterproofed)
258 could be left in the field in time lapse mode for long periods at a time, even relaying
259 imagery over the internet in real-time if communications are available. Overall,
260 moving forward there are many advantages to using the Raspberry Pi, however the
261 key conclusion is that a fit for purpose and dynamic solution for the collection of
262 hemispherical imagery can be readily produced at a low cost.

263 **Acknowledgements**

264 Funding for this research was provided by the Rail Safety and Standards Board
265 (RSSB) and the Engineering and Physical Sciences Research Council (EPSRC).

266 **References**

- 267 1. **Anderson, M.C.** 1964: Studies of Woodland light climate. *Journal of Ecology*
268 52, 27-41
- 269 2. **Baret, F.** and **Agroparc, S.** 2004: A simple method to calibrate hemispherical
270 photographs. INRA-CSE, France
271 (http://147.100.66.194/can_eye/hemis_calib3.pdf).
- 272 3. **Bréda, N. J.** 2003: Ground-based measurements of leaf area index: a review
273 of methods, instruments and current controversies. *Journal of experimental*
274 *botany*, 54(392), 2403-2417
- 275 4. **Chapman, L.** 2008: An introduction to upside-down remote sensing, *Progress*
276 *in Physical Geography* 32 (5), 529-542
- 277 5. **Chapman, L.** 2007: Potential applications of near infra-red hemispherical
278 imagery in forest environments. *Journal of Agricultural and Forest*
279 *Meteorology*, 143(1), 151-156.

- 280 6. **Chapman, L., Thornes, J. E., Muller, J. P., and McMuldroy, S.** 2007:
281 Potential applications of thermal fisheye imagery in urban environments. *IEEE*
282 *Geoscience and Remote Sensing Letters*, 4(1), 56-59.
- 283 7. **Chen, J. M.** 1996: Optically-based methods for measuring seasonal variation
284 of leaf area index in boreal conifer stands. *Journal of Agricultural and Forest*
285 *Meteorology*, 80(2-4), 135-163.
- 286 8. **Duveiller, G., and Defourny, P.** 2010: Batch processing of hemispherical
287 photography using object-based image analysis to derive canopy biophysical
288 variables. *Proceedings of GEOBIA*, 1682-1777.
- 289 9. **Chianucci, F, Leonardo D, Donatella G, Daniele B, Vanni N, Cinzia L,**
290 **Andrea R and Piermaria C** 2016: "Estimation of canopy attributes in beech
291 forests using true colour digital images from a small fixed-wing
292 UAV." *International journal of applied earth observation and*
293 *geoinformation* 47. 60-68.
- 294 10. **Chianucci, F., Macfarlane, C., Pisek, J., Cutini, A., and Casa, R.** 2015:
295 Estimation of foliage clumping from the LAI-2000 Plant Canopy Analyzer:
296 effect of view caps. *Trees*, 29(2), 355-366.
- 297 11. **Danson, F. M., Hetherington, D., Morsdorf, F., Koetz, B., and Allgower, B.**
298 2007: Forest canopy gap fraction from terrestrial laser scanning. *IEEE*
299 *Geoscience and remote sensing letters*, 4(1), 157-160.
- 300 12. **Englund, S. R., O'brien, J. J., and Clark, D. B.** 2000: Evaluation of digital
301 and film hemispherical photography and spherical densiometry for measuring
302 forest light environments. *Canadian Journal of Forest Research*, 30(12),
303 1999-2005.

- 304 13. **Delta** 2017: HemiView Forest Canopy Image Analysis System,
305 <https://www.delta-t.co.uk/product/hemiview/> accessed 30/01/2018
- 306 14. **Frazer, G. W., Fournier, R. A., Trofymow, J. A., and Hall, R. J.** 2001: A
307 comparison of digital and film fisheye photography for analysis of forest
308 canopy structure and gap light transmission. *Journal of Agricultural and forest*
309 *meteorology*, 109(4), 249-263.
- 310 15. **Garrigues, S., Shabanov, N. V., Swanson, K., Morissette, J. T., Baret, F.,**
311 **and Myneni, R. B.** 2008: Intercomparison and sensitivity analysis of Leaf
312 Area Index retrievals from LAI-2000, AccuPAR, and digital hemispherical
313 photography over croplands. *Journal of Agricultural and Forest meteorology*,
314 148(8), 1193-1209.
- 315 16. **Grimmond, C. S. B., Potter, S. K., Zutter, H. N., and Souch, C.** 2001: RaPid
316 methods to estimate sky-view factors applied to urban areas. *International*
317 *Journal of Climatology*, 21(7), 903-913
- 318 17. **Göteborg Urban Climate Group**, 2018: Sky-view Calculator, University of
319 Göthenburg, [https://gvc.gu.se/english/research/climate/urban-](https://gvc.gu.se/english/research/climate/urban-climate/software/download)
320 [climate/software/download](https://gvc.gu.se/english/research/climate/urban-climate/software/download). Accessed 30/01/2018
- 321 18. **Hale, S. E., and Edwards, C.** 2002: Comparison of film and digital
322 hemispherical photography across a wide range of canopy densities. *Journal*
323 *of Agricultural and Forest Meteorology*, 112(1), 51-56.
- 324 19. **Hall, R. J., Fournier, R. A., and Rich, P.** 2017: Introduction. In Hemispherical
325 Photography in Forest Science: *Theory, Methods, Applications* (pp. 1-13).
326 Springer Netherlands.

- 327 20. **Holmer, B., Postgård, U. and Eriksson, M.**, 2001: Sky view factors in forest
328 canopies calculated with IDRISI. *Theoretical and Applied Climatology*, 68(1),
329 pp.33-40.
- 330 21. **Homolová, L., Malenovský, Z., Hanuš, J., Tomášková, I., Dvořáková, M.,**
331 **and Pokorný, R.** 2007: Comparaison of different ground techniques to map
332 leaf area index of Norway spruce forest canopy. *In Proceedings of the*
333 *International Society for Photogrammetry and Remote Sensing (ISPRS)*
- 334 22. **Hu, L., Gong, Z., Li, J., and Zhu, J.** 2009: Estimation of canopy gap size and
335 gap shape using a hemispherical photograph. *Trees*, 23(5), 1101-1108.
- 336 23. **Ishida, M.** 2004: Automatic thresholding for digital hemispherical
337 photography. *Canadian Journal of Forest Research*, 34(11), 2208-2216.
- 338 24. **Johnson, G. T., and Watson, I. D.** 1984: The determination of view-factors in
339 urban canyons. *Journal of Climate and Applied Meteorology*, 23(2), 329-335.
- 340 25. **Jonckheere, I., Fleck, S., Nackaerts, K., Muys, B., CopPin, P., Weiss, M.,**
341 **and Baret, F.** 2004: Review of methods for in situ leaf area index
342 determination: Part I. Theories, sensors and hemispherical photography.
343 *Journal of Agricultural and Forest meteorology*, 121(1), 19-35.
- 344 26. **Kelley, C.E. and Krueger, W.C.**, 2005: Canopy cover and shade
345 determinations in riparian zones. *Journal of the American Water Resources*
346 *Association*, 41(1), pp.37-046.
- 347 27. **Lang, M., Kuusk, A., Möttus, M., Rautiainen, M., and Nilson, T.** 2010:
348 Canopy gap fraction estimation from digital hemispherical images using sky
349 radiance models and a linear conversion method. *Journal of Agricultural and*
350 *Forest Meteorology*, 150(1), 20-29.

- 351 28. **Leblanc, S. G., Chen, J. M., Fernandes, R., Deering, D. W., and Conley, A.**
352 2005: Methodology comparison for canopy structure parameters extraction
353 from digital hemispherical photography in boreal forests. *Journal of*
354 *Agricultural and Forest Meteorology*, 129(3),187-207.
- 355 29. **Lindberg, F., and Holmer, B.** 2010: Sky View Factor Calculator, Göteborg
356 Urban Climate Group, Department of Earth Sciences, University of
357 Gothenburg
- 358 30. **Liu, Z., Wang, C., Chen, J. M., Wang, X., and Jin, G.** 2015: Empirical
359 models for tracing seasonal changes in leaf area index in deciduous broadleaf
360 forests by digital hemispherical photography. *Journal of Forest Ecology and*
361 *Management*, 351, 67-77.
- 362 31. **Nikon**, CoolPix 4500 product archive, 2017:
363 <http://imaging.nikon.com/lineup/CoolPix/others/4500/> accessed 30/01/2018
- 364 32. **Raspberry Pi** 2016: <https://www.RaspberryPi.org/products/Pi-noir-camera/>,
365 Accessed 2017
- 366 33. **Rich, P. M.** 1990: Characterizing plant canopies with hemispherical
367 photographs. *Remote sensing reviews*, 5(1), 13-29.
- 368 34. **Ringold, P. L., Sickle, J., Rasar, K., and Schacher, J.** 2003: Use of
369 hemispheric imagery for estimating stream solar exposure. *Journal of the*
370 *American Water Resources Association*, 39(6), 1373-1384.
- 371 35. **Schwalbe, E., Maas, H. G., Kenter, M., and Wagner, S.** 2009: Hemispheric
372 image modeling and analysis techniques for solar radiation determination in
373 forest ecosystems. *Journal of Photogrammetric Engineering and Remote*
374 *Sensing*, 75(4), 375-384.

- 375 **36. Steyn, D.G.**, 1980: The calculation of view factors from fisheye-lens
376 photographs: Research note.
- 377 **37. Turner, D. P., Cohen, W. B., Kennedy, R. E., Fassnacht, K. S., and Briggs,**
378 **J. M.** 1999: Relationships between leaf area index and Landsat TM spectral
379 vegetation indices across three temperate zone sites. *Remote sensing of*
380 *environment*, 70(1), 52-68.
- 381 **38. Urquhart, B., Kurtz, B., Dahlin, E., Ghonima, M., Shields, J. E., and**
382 **Kleissl, J.** 2014: Development of a sky imaging system for short-term solar
383 power forecasting. *Atmospheric Measurement Techniques Discussions*, 7,
384 4859-4907.
- 385 **39. Wagner, S., and Hagemeier, M.** 2006: Method of segmentation affects leaf
386 inclination angle estimation in hemispherical photography. *Journal of*
387 *Agricultural and Forest Meteorology*, 139(1), 12-24.
- 388 **40. Watson, I. D., and Johnson, G. T.** 1987: Graphical estimation of sky view-
389 factors in urban environments. *Journal of Climatology*, 7(2), 193-197.
- 390 **41. Zhang, Y., Chen, J.M. and Miller, J.R.,** 2005: Determining digital
391 hemispherical photograph exposure for leaf area index estimation. *Agricultural*
392 *and Forest Meteorology*, 133(1-4), pp.166-181.
- 393